Int. J. Radiation Oncology Biol. Phys., Vol. ■, No. ■, pp. 1–9, 2010

0360-3016/10/$–see front matter

ELSEVIER

doi:10.1016/j.ijrobp.2009.11.030

PHYSICS CONTRIBUTION

PATIENT MOTION AND TARGETING ACCURACY IN ROBOTIC SPINAL RADIOSURGERY: 260 SINGLE-FRACTION FIDUCIAL-FREE CASES

CHRISTOPH FÜRWEGER, PH.D.,* CHRISTIAN DREXLER,* MARKUS KUFELD, M.D.,* ALEXANDER MUACEVIC, M.D.,* BERNDT WOWRA, M.D.,* AND ALEXANDER SCHLAEFER, PH.D.†

*European Cyberknife Center, Munich, and †University of Luebeck, Institute for Robotics and Cognitive Systems, Luebeck, Germany

Purpose: To evaluate clinical targeting precision and assess patient movement data during fiducial-free, single-fraction spinal radiosurgery with the Cyberknife (CK).

Methods and Materials: Image-guided spine tracking accuracy was tested using two phantoms. Movement patterns (three translations, roll, pitch and yaw) were obtained from log files of 260 patient treatments (47 cervical, 89 thoracic, 90 lumbar, and 34 pelvic/sacral). For two treatments (average and maximum motion scenario), we added offsets to all beams according to recorded patient movements and recalculated the delivered dose distribution to simulate the dosimetric impact of intrafraction motion.

Results: Phantom spine position was registered with an accuracy of <0.2 mm for translational and <0.3° for rotational directions. Residual patient motion yielded mean targeting errors per beam of 0.28 ± 0.13 mm (X), 0.25 ± 0.15 mm (Y), 0.19 ± 0.11 mm (Z) and 0.40 ± 0.20° (roll), 0.20 ± 0.08° (pitch), and 0.19 ± 0.08° (yaw). Spine region had little influence on overall targeting error, which was <1 mm for more than 95% of treatments (median, 0.48 mm). In the maximum motion case, target coverage decreased by 1.7% (from 92.1% to 90.4%) for the 20-Gy prescription isodose. Spinal cord volume receiving more than 8 Gy increased slightly, from 2.41 to 2.46 cm^3.

Conclusions: Submillimeter targeting precision was obtained for fiducial-free spinal radiosurgery despite patient motion. Patient motion has little effect on the delivered dose distribution when image-guided correction of beam aiming is employed. © 2010 Elsevier Inc.

Spinal radiosurgery, Spine, Fiducial free registration, Intrafraction motion, Cyberknife.

INTRODUCTION

Image-guidance techniques for radiosurgery are intended to minimize targeting error as the patient's position deviates from the planning computer tomography (CT) images. Both inter- and intrafraction motion contribute to the overall geometric error in treatment delivery (1–4). Image-guided patient setup can minimize the impact of interfraction motion, but efforts to monitor and compensate for intrafraction motion are still limited (5, 6).

The Cyberknife (CK) is a frameless, robotic radiosurgery system that uses a stereoscopic kV imaging system for image guidance. The patient is positioned on a motorized treatment couch between two amorphous silicon detectors and ceiling-mounted diagnostic X-ray sources. During treatment, the linac is moved in a large solid angle around the patient, delivering beams from more than 100 noncoplanar directions. Dual X-ray images acquired during treatment are compared with digitally reconstructed radiographs (DRRs) generated from the treatment planning CT scan. The position and orientation of the vertebral target is identified by image-to-image registration (7). Calculated translational and rotational offsets of the spine are used to reposition the linac head to align incident beams to the target position. In this manner, patient position is tracked throughout the entire treatment.

At our institution, we treat spinal lesions with the CK using a single-fraction, fiducial-free concept (8). High doses (~20 Gy) and long treatment times (over 1 hour) make frequent image-guided compensation of intrafraction motion crucial. Patient motion between imaging acquisitions, however, is not detected and causes a misalignment error of each beam with respect to the target, which is superposed on the error resulting from the accuracy limits of the CK tracking system. We assessed the contribution of this residual motion to overall targeting error in spinal treatments with the CK. The accuracy of the spine-tracking system itself was determined in phantom experiments so that the unique contribution of residual patient motion to overall tracking accuracy could be estimated. We analyzed data from 260 spinal treatments. A conservative measure of total targeting error was derived and expressed relative to the treated spinal section.

Reprint requests to: Christoph Fürweger, Ph.D., Max-Lebsche-Platz 31, 81377 Munich, Germany. Tel: (+49) 89-452336-0; Fax: (+49) 89-452336-16; E-mail: christoph.fuerweger@cyber-knife.net

Conflict of interest: none.

Acknowledgment—We thank David Schaal and Warren Kilby, Accuray Incorporated, for editorial support.

Received July 3, 2009, and in revised form Oct 19, 2009. Accepted for publication Nov 23, 2009.

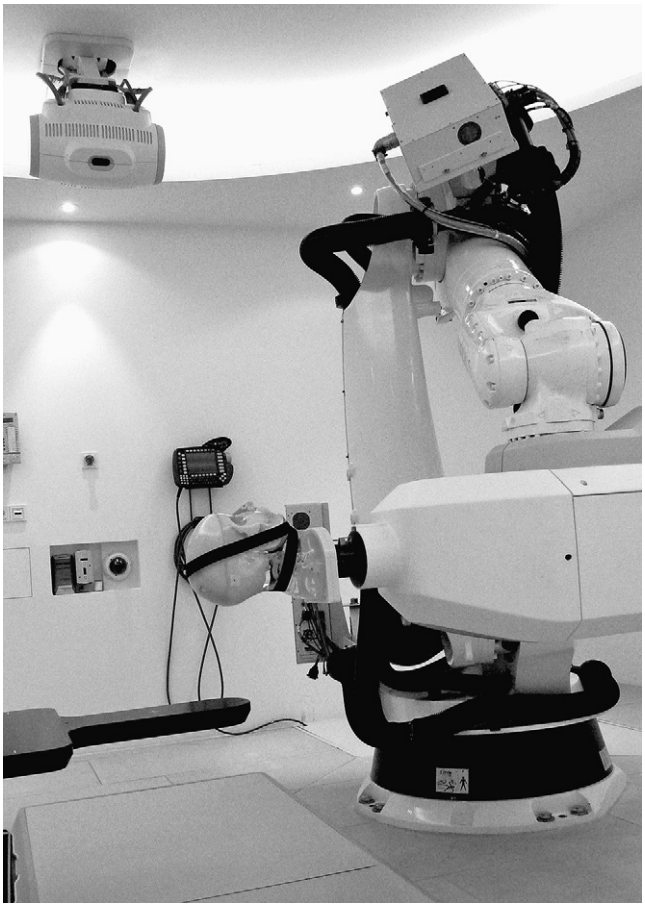

Fig. 1. Setup for cervical spine tracking tests: An anthropomorphic head-and-neck phantom is firmly attached to the nozzle of the Cyberknife linac head. The manipulator positions the cervical spine section at predefined points in the frame of reference of the image-guidance system.

The impact of residual motion on the planned dose distribution, target coverage, and dose deposited in organs at risk were determined for representative cases.

METHODS AND MATERIALS

Phantom tests: Accuracy of the tracking system

Spine tracking was tested on two phantoms with our CK (Generation 4: on-floor X-ray detectors, 1024 × 1024 pixel matrix). An anthropomorphic head and neck phantom with seven cervical vertebrae was CT-scanned with a slice thickness of 1 mm. This CT data set was used to calculate reference DRRs. The phantom was firmly attached to the linac head, and the manipulator (the robot holding the linac) was used to position (specified repeatability: ± 0.12 mm) the phantom precisely in the imaging frame (Fig. 1). The cervical spine section of the phantom was used as tracking target. Translational and rotational offsets of the phantom were introduced by repositioning of the six robot joints. The correlation of live images with reference DRRs in six (three translational and three rotational) dimensions was assessed.

Thoracic vertebrae tracking was tested with a thorax phantom. After CT scanning, the phantom was positioned on the treatment couch (accuracy: ±0.3 mm). The phantom was moved in three translational and two rotational (roll and pitch) directions by remotely controlling the couch.

Phantom tests covered the range of patient movement that can be compensated for automatically (*i.e.,* without couch correction) by the CK system (10 mm in translations, 1° in roll and pitch, 3° in yaw from the reference position). Nominal translational positions were ±10, ±6, ±2, and 0 mm. Rotational steps were 0.15° (roll), 0.25° (pitch), and 0.5° (yaw) for cervical spine over that range. Because of the lower couch accuracy, larger steps of 0.5° were selected for thoracic spine roll and pitch.

Four standard treatments were delivered to the cervical spine of the head-and-neck phantom. The targeting error was calculated according to the patient treatment formalism in the following section to establish a baseline for a nonmoving patient.

Analysis of residual patient motion

We analyzed 260 single-fraction spine treatments. Patients were treated in the supine position for a median treatment time of 90 min. Thermoplastic masks were applied for treatments of the upper cervical spine. Knee rests and cushions were used for comfort. No additional immobilization devices were applied. Dose planning and DRR generation were based on a CT scan with 1-mm slice thickness. On average, 171 beams were delivered per treatment, and X-ray images were acquired every 1.5 min.

For each image acquisition, the deviation in position and orientation between the tracked spinal area of interest, and the reference image is immediately determined by image-to-image-registration. These offsets are calculated as 6-dimensional vectors d that consist of three translational (X, Y, Z [superior/inferior, left/right, anterior/posterior] and three rotational components (ϕ, θ, and ξ [roll, pitch, yaw]), which are recorded in a treatment log file. The robot uses the most recent values for an online correction of the linac position and angle before beam delivery.

Patient motion between image acquisitions is reflected by the difference of two successive vectors, d_n and d_{n+1}. We attribute this difference as a targeting error Δ to each individual beam i delivered between the imaging step n and n+1 as:

$$\Delta_i = d_{n+1} - d_n = (\Delta x_i\ \Delta y_i\ \Delta z_i\ \Delta\varphi_i\ \Delta\phi_i\ \Delta\xi_i) \qquad (1)$$

By this definition, the targeting error includes the statistical error of the imaging system, which for a specific image pair cannot be determined separately in an analysis of patient treatment data. To illustrate, if the imaging system detects a displacement of 0 mm along the x axis for imaging step n and 0.5 mm for imaging step n+1 with three beams delivered in between, we attribute a targeting error of 0.5 mm in X direction to all three beams. This consistently overestimates a monotonous drift with a small stochastic component (see Fig. 2). Predominant stochastic motion can lead to an underestimate for part of the time between image acquisitions.

The data were corrected for couch movement and treatment interruptions (*e.g.,* due to breaks requested by the patient), identified using the timestamp of the acquired images. In this manner, a distribution of the targeting error and a treatment average error in all 6 degrees of freedom were determined for each patient.

Roll, pitch, and yaw errors refer to different rotations of the patient around the predefined tracking center of the patient CT (CTC) with respect to the incoming beam. Therefore, the geometric targeting error caused by a rotational offset of the patient depends mainly on the location of the target with regard to the CTC. The target vector $r = (x, y, z)$ shall be defined as the vector from the CTC to arbitrary target coordinates. The vector $r' = (x', y', z')$ corresponds to the vector r after a translational shift and a rotation of the patient

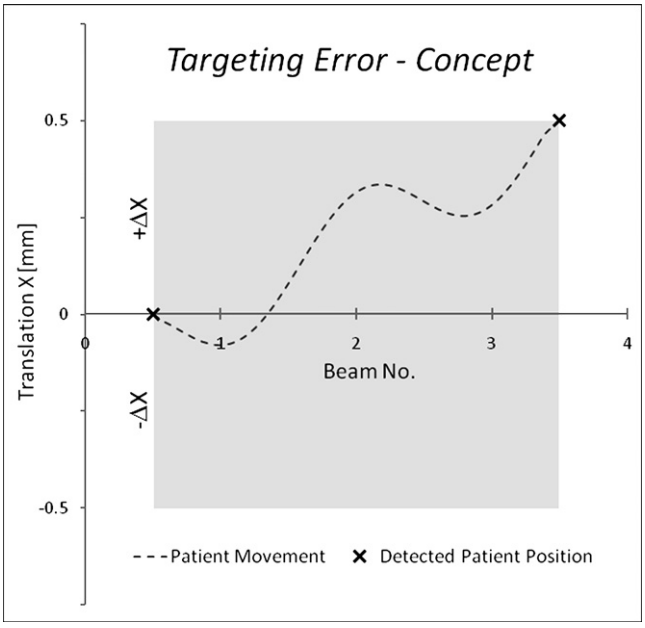

Fig. 2. The concept for calculation of the targeting error (translational direction X): The patient position is identified at two time points (indicated by a cross) and moves in an unknown course of movement while three beams are delivered in between. The positional difference ΔX is used as a measure for the targeting error.

frame of reference around the CTC. It can be shown (9) that for small angles, this transformation can be approximated in a simple manner by

$$r' = \boldsymbol{M} \times \boldsymbol{r} + \Delta \boldsymbol{t}, \tag{2}$$

with translational shift Δt = (Δx, Δy, Δz) and matrix M given by

$$\boldsymbol{M} = \begin{pmatrix} 1 & \Delta\theta & -\Delta\xi \\ -\Delta\theta & 1 & \Delta\varphi \\ \Delta\xi & -\Delta\varphi & 1 \end{pmatrix}, \tag{3}$$

whereby $\Delta\phi$, $\Delta\theta$ and $\Delta\xi$ refer to roll, pitch, and yaw shifts in radian.

We introduce a single quality measure that describes the impact of residual patient motion on the precision of the treatment delivery. As a simplification, all beams are assumed to be directed at the maximum dose point (reference point), which is located in the target for all our treatments. Thus, the vector R from the CTC to the maximum dose point (mean length: 2.4 cm for spinal cases) can be used as a single, representative target vector for all beams. The absolute targeting error e_i of beam i is then given by

$$e_i = |R' - R| = |\boldsymbol{M}_i \times R + \Delta t_i - R|, \tag{4}$$

with M_i as the specific transformation matrix for each beam. For every treatment, we generated the mean value of this absolute targeting error by averaging overall delivered beams.

The 260 treatments included cervical (47), thoracic (89), lumbar (90), and pelvic (34) treatments. The pelvic group contained all treatments of pelvic and sacral lesions with a distance of greater than 6 cm (mean: 12.4 cm) from the CTC, which was located in the lumbar vertebrae 4 or 5. For the other groups, the CTC was commonly defined by the user to be located within the treated vertebral body. Means and standard errors for each group were calculated to investigate the dependence of the targeting error on the tracked spine section.

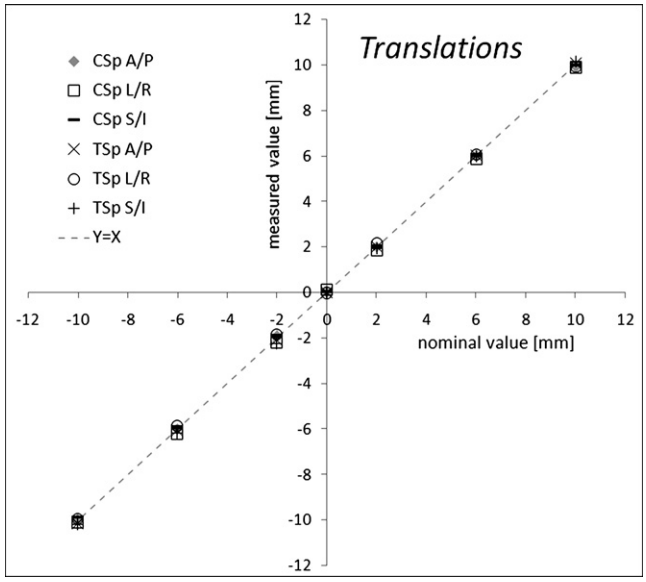

Fig. 3. Phantom tests: translational tracking accuracy of the cervical (CSp) and thoracic (TSp) spine. Results are means of 10 measurements. Standard deviations (~0.1 mm) are omitted for readability.

Impact of residual patient motion on the dose distribution

The CK treatment planning system stores beam information for each plan, including source and target vectors s_i and t_i for each individual beam i. We added translational and rotational targeting errors resulting from our analysis of imaging data to each individual beam. A new beamset was generated by calculating shifted and rotated source and target vectors s'_i and t'_i according to equation (2). In the plan file, the original beamset was replaced using these transformed beam coordinates. Dose distributions were calculated using Monte Carlo dose calculation with the statistical uncertainty set to be less than 0.2% in high dose areas. Quantitative changes in the dose distribution caused by patient motion were analyzed on the basis of dose–volume histograms of the target and adjacent critical structures.

RESULTS

Phantom measurements

For the three translational directions, the CK system showed a linear response over the whole range (–10 to +10 mm) when tracking the phantom cervical spine (Fig. 3). All measured mean values deviated from the nominal, robot-induced offsets by less than 0.2 mm. Given the standard deviation of approximately 0.1 mm and the robot repeatability of 0.12 mm, it can be concluded that the translational spine position is correctly detected without systematic errors within the limits of our measurement technique. The couch-based tracking tests with the thorax phantom confirmed these results, allowing for the slightly greater uncertainty of phantom positioning by the couch (<0.3 mm).

Detection of rotational shifts of the phantom spine depended on the direction of rotation (Fig. 4a–c). Mean values for cervical spine yaw were off by less than 0.12° over the observed range of –5° to +5°, with standard deviations of less than 0.15°, which is within the detection limits of our test setup. Cervical and thoracic sections show consistent results

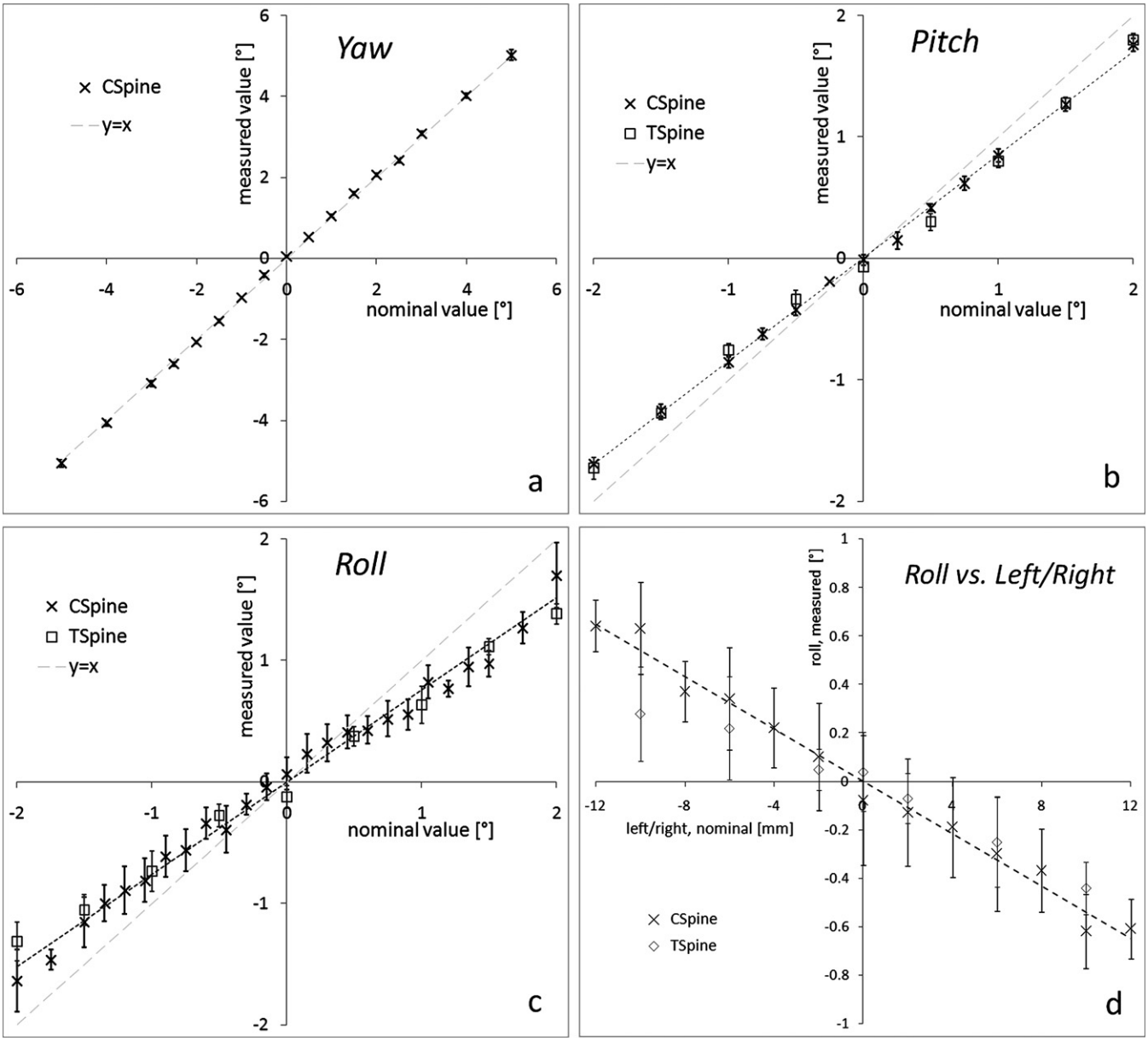

Fig. 4. Phantom tests: tracking accuracy of cervical spine (CSp) yaw (a), cervical and thoracic spine (TSp) pitch (b), and roll (c). Detected roll offsets (nominal roll: 0°) as a function of left/right displacements of the phantom (d). Results are means of 10+ measurements ± SD.

for pitch: the Xsight spine-tracking system slightly underestimated absolute deviations from the reference position across the observed range, reaching approximately 0.15° for a nominal value of ±1° pitch, which is slightly larger than the standard deviation of <0.1° for our pitch measurements.

For both phantoms, the measured roll values showed much larger standard deviations, up to 0.2°, than those obtained for the other orientations for the [–1°; +1°] interval. On average, absolute nominal roll deviations were systematically underestimated by approximately 25%. Therefore, in the most important range [–1°; +1°], this systematic error is either smaller or approximates the statistical uncertainty. Hence, it is reasonable to refrain from a systematic correction of patient roll data.

For combined translational and rotational shifts of the cervical spine, no cross-relation for anterior/posterior (A/P), superior/inferior (S/I), pitch and yaw directions was found. However, left/right (L/R) displacements of the phantom led to an incorrect detection of roll offsets by the CK target locating system (Fig. 4d). For a left/right offset of ±10 mm and a nominal value of 0° roll, a roll misalignment of approximately ±0.5° was detected. This effect is negligible for offsets up to 2 mm when compared with the statistical uncertainty of roll detection.

The analysis of offsets for four cervical spine treatments of a nonmoving phantom yielded a translational targeting error of 0.05 ± 0.01 mm for L/R and A/P and a slightly lower value of 0.02 ± 0.01 mm for I/S. The rotational errors were found

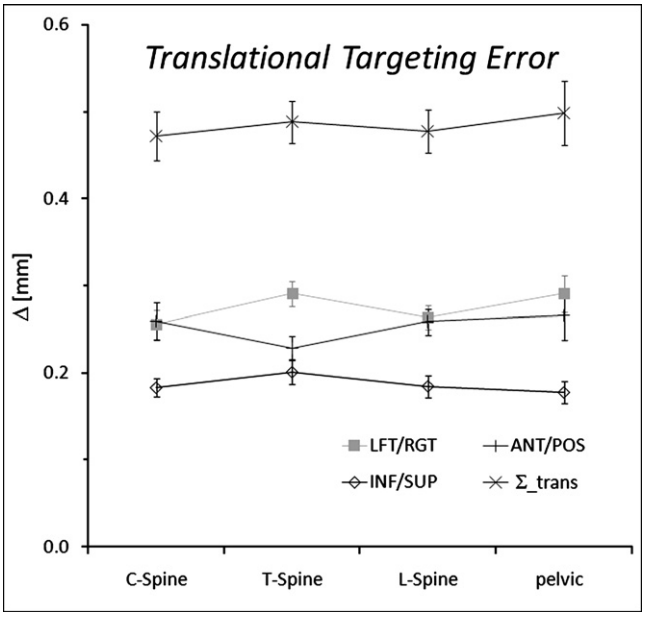

Fig. 5. Patient motion: translational targeting errors (left/right (LFT/RGT), anterior/posterior (ANT/POS), inferior/superior (INF/SUP), and radial) depending on the target location. Results are means of the respective treatment group ± standard error.

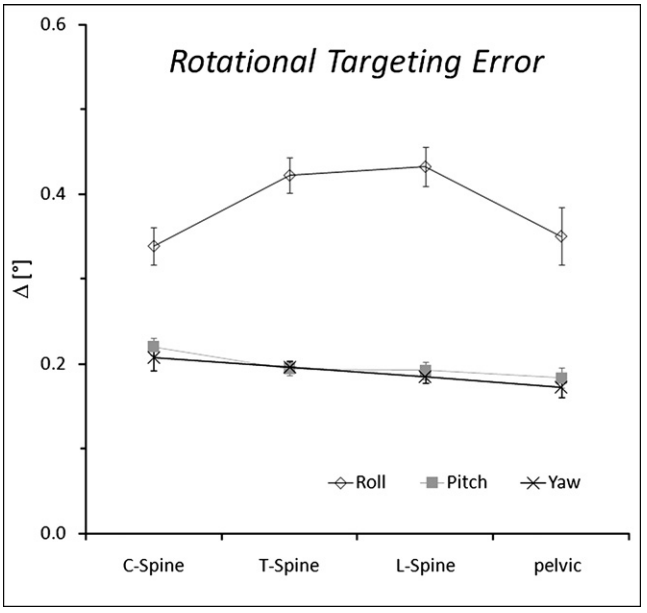

Fig. 6. Patient motion: rotational targeting errors (roll, pitch and yaw) depending on the target location. Results are means of the respective treatment group ± standard error. C = cervical; T = thoracic; L = lumbar.

to be 0.11° ± 0.03° for roll, 0.04° ± 0.01° for pitch and 0.05° ± 0.01° for yaw. A total targeting error of 0.10 ± 0.02 mm was determined.

Residual patient motion—the targeting error

Translations. In total, the translational component of patient motion caused an almost constant average radial targeting error of approximately 0.5 mm (Fig. 5) for all treatment groups. Movement in I/S direction contributed least (∼0.2 mm). L/R and A/P shifts resulted in a targeting error of the same magnitude for cervical, lumbar, and pelvic/sacral lesions (0.25 to 0.3 mm).

Pitch and yaw. Shifts in pitch and yaw directions were almost identical (Fig. 6): on average, the contribution was greatest in cervical spine treatments (0.22 ± 0.01° pitch and 0.21 ± 0.02° yaw) and decreased slightly for lower spinal sections.

Roll. The targeting error due to roll was twice as high as for the other axes (Fig. 6). The roll deviations for thoracic and lumbar treatments were significantly higher (0.42 and 0.43 ± 0.02°) than for cervical (0.34 ± 0.02°) and pelvic lesions (0.35 ± 0.03°). However, because the CTCs for both lumbar and pelvic treatments are located in the lumbar spine section, similar values for roll are to be expected. A more refined analysis of the combined roll data (Fig. 7) shows that the position of the CTC (or the target, respectively) within the lumbar spine has a major impact on roll movement. Consistent with the notion that the location of the CTC is a determinant of observed roll motion, roll is equally stable for pelvic targets and treatments of the lumbar vertebrae 4 and 5. Patient roll movement reached a maximum (0.45–0.5°) for lesions in the spine section between the 11th thoracic and the 2nd lumbar vertebral body. Furthermore, the amount of roll was found to increase continually from low values for the upper cervical vertebrae (∼0.3°) up to this maximum. Pitch and yaw rotations did not show significant differences over the range of targeted vertebrae.

Total targeting error. The mean total targeting error includes both translations and the impact of rotations

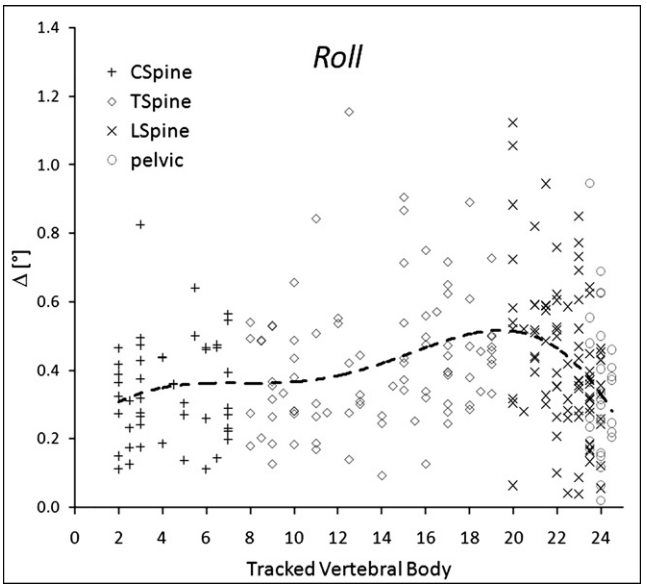

Fig. 7. Patient motion: the targeting error due to roll movement depending on the tracked vertebral body. Each data point corresponds to the mean roll error of an individual treatment. The data is fitted with a sixth-degree polynomial. C = cervical; T = thoracic; L = lumbar.

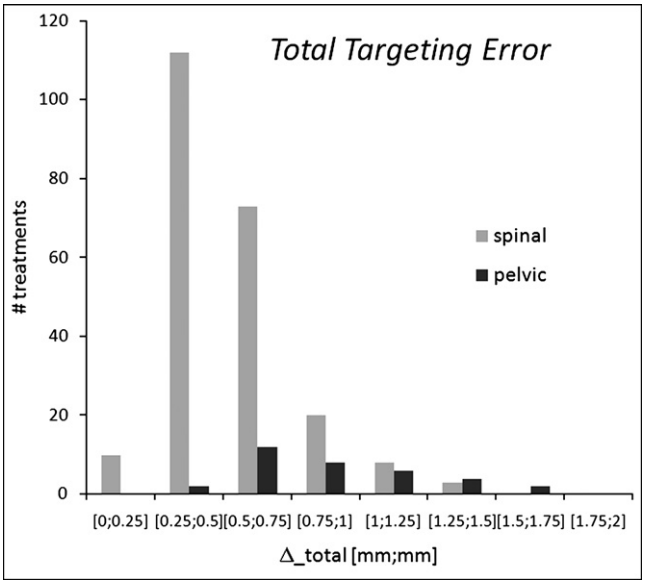

Fig. 8. Patient motion: the distribution of the total targeting error for treatments of spinal lesions and distant pelvic targets.

depending on target position (Fig. 8). For more than 95% of our cervical, thoracic, and lumbar treatments, this error was <1 mm, and the median error was 0.48 mm. The pelvic/sacral treatments are subject to a higher error (median, 0.92 mm) because of the amplification of rotational shifts due to the larger distance between the lesion and the CTC.

The impact on the dose distribution

We analyzed a maximum motion case with a mean total targeting error >1 mm, drawn from the 5% of treatments with the largest errors, and an average case, with targeting errors at or slightly above the median for all six directions. Both lesions were within approximately 2 mm of the myelon to demonstrate the impact of patient motion on an organ at risk. In both cases, 20 Gy was applied to the 65% isodose line. For dose–volume histogram analysis, the spinal cord was contoured along the lesion and extended by 1 cm in the superior and the inferior direction. The treatment parameters and the determined targeting errors are given in Table 1.

For maximum motion a slight deformation of the dose distribution (Fig. 9), and a decrease in target coverage from 92.1 to 90.4% for the 20 Gy isodose line were obtained. The spinal cord volume receiving more than 8 Gy increased from 2.41 to 2.46 cm^3. In the average-motion case, the dose distribution was visually unchanged by residual motion (Fig. 10). Target coverage was decreased by 0.6%, and the spinal cord volume receiving more than 8 Gy increased by 0.01 cm^3.

DISCUSSION

Fiducial-free spine tracking accuracy

For the ideal phantom case, our tests revealed a tracking precision of $<0.2 \pm 0.1$ mm for each translational direction with no evidence of a systematic error. To achieve a comparable precision with fiducial-based image guidance, a common, well-established standard in spinal radiosurgery (10, 11), three or more fiducials have to be implanted when a small perturbation of 0.1 mm for the position of an individual fiducial is assumed (12). Because fiducial tracking requires invasive implantation, our tracking test results strongly argue for treating spinal lesions with CK skeletal structure tracking.

We found that only large translational offsets in L/R direction were partly misinterpreted as roll shifts of up to 0.5°. No systematic errors were determined for the phantom being within 2 mm from the centered position in any translational direction. At our center, it is common practice to minimize patient offsets before treatment to be less than 1 mm. Furthermore, we manually interrupt the treatment and correct the patient position when offsets larger than 2 mm are encountered. With this practice, systematic roll registration errors have no impact on treatment delivery quality.

Spine deformation may possibly affect targeting accuracy. CK spine tracking uses a hierarchical mesh algorithm, allowing for deformation (7). This mesh typically covers three adjacent vertebrae, which restricts the extent of deformation. However, given the limitation in our study of rigid phantoms, we cannot quantify the potential impact on targeting.

Targeting error due to patient motion

We have stressed that the targeting errors due to residual motion and statistical error cannot be separated in an analysis that is solely based on tracking data from patient treatments. However, the targeting error of 0.1 mm for a cervical spine treatment of a stationary phantom reflects mistargeting purely due to the statistical error of the tracking system. This error accounts for less than 20% of the total targeting error due to residual motion for an average patient treatment. This is evidence that the predominant fraction of the targeting error in patient treatments results from actual motion and not from the measurement uncertainty of the CK image-guidance system.

Until now, studies of intrafraction patient motion in spinal treatments (1, 3, 4, 9, 13–16) have been based on, at most, 23

Table 1. The impact of patient motion on the dose distribution: treatment and dose–volume histogram characteristics

Case	Motion	Total targeting error [mm]	No. Beams	Coverage 20 Gy [%]		Spinal cord vol. >8 Gy [ccm]	
				Planned	Delivered	Planned	Delivered
1	Extensive	1.17	167	92.1	90.4	2.41	2.46
2	Average	0.61	181	97.4	96.8	2.40	2.41

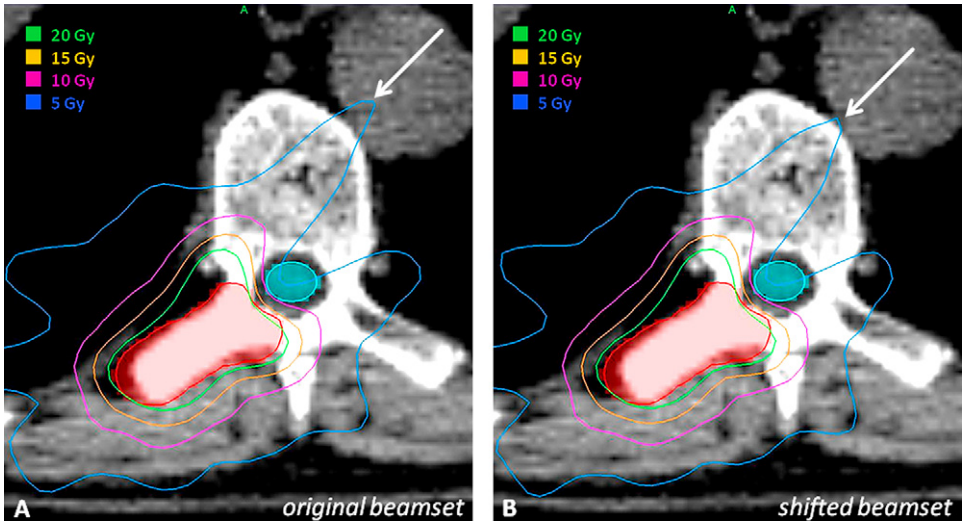

Fig. 9. Maximum residual patient motion: the dose distribution due to the (''shifted'') beamset with applied offsets (B) is compared with the originally planned dose distribution (A). The target (red) and the spinal cord (light blue) are indicated. The lower isodose lines show visible differences, as indicated by the arrow.

cases. Because intrafraction motion is highly patient-specific, the statistical significance of results is limited when only small patient numbers are considered. For this reason, we analyzed 260 cases to gain statistical power.

Hoogeman *et al*. (14) studied patient motion patterns in 11 CK spine treatments with fiducial implants. In some cases, displacements of the patient exceeded 1 mm within a 3-min time span. Kim *et al*. (15) measured the position of the spine using the cone-beam CT of an Elekta system before and after nine single-fraction treatments with an average duration of 40 min. They reported an average translational difference in the target position of 1.8 $\pm$ 1.0 mm and a total rotational misalignment of up to 6°. Agazaryan *et al*. (1), using a Novalis system, found patient movement of up to 3 mm along each axis within a 5-min time span despite patient immobilization. These studies show that a targeting error of several millimeters due to patient motion is to be expected if the target position is not monitored and corrected for during treatment. We have demonstrated that a mean residual targeting error of less than 1 mm can be consistently achieved by monitoring the target position and adapting beam direction in 1.5-min intervals. This is feasible with only minimal immobilization measures, and even with long treatment times.

For finite time intervals, patient motion patterns are known to resemble a monotonous ''drift'' overlaid by a stochastic component (14). Our error calculation overestimates drift but can underestimate stochastic motion between image acquisitions. This stochastic component leads to misses in random directions. Because of the large number of beams delivered in a typical treatment, an offset of one beam can be partly compensated by another with a different offset, so the deviation due to statistical mistargeting tends to average

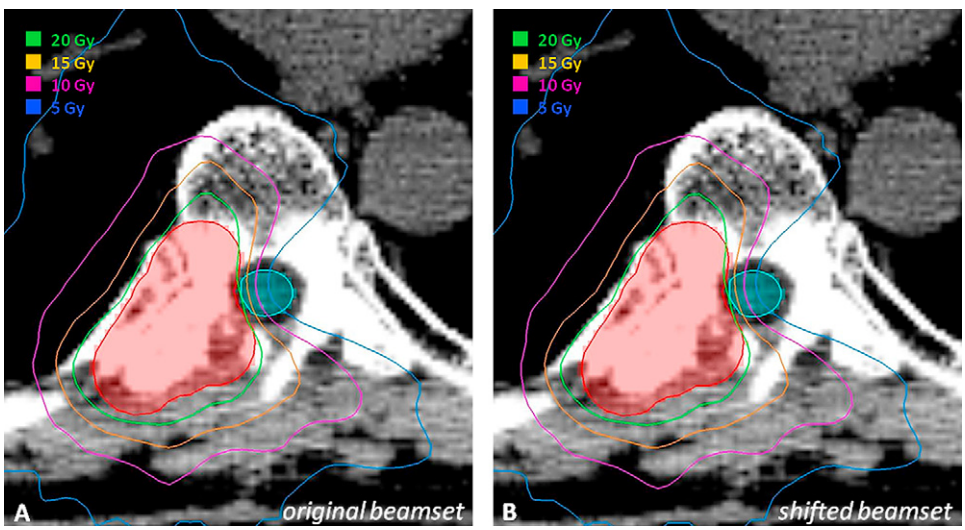

Fig. 10. Average residual patient motion: the dose distribution due to the (''shifted'') beamset with applied offsets (B) is compared with the originally planned dose distribution (A). The target (red) and the spinal cord (light blue) are indicated. The shape of the isodose lines is visually identical.

out and has a reduced impact on the delivered dose distribution.

On average, we determined a radial offset of 0.53 mm due to residual motion for spinal targets. Considering a mean imaging interval of 1.5 min, this value is in good agreement with the data published by Hoogeman *et al*. (14). Murphy *et al*. (16) analyzed 23 spinal cases with fiducial or skeletal tracking. They found a mean radial offset of 0.89 mm for cervical and 0.86 mm for thoracic/lumbar treatments. Although essential information on these spine cases, such as CT slice spacing, was not provided, and the position measurements of all but two cases were limited to translations only, the data of Murphy *et al*. nevertheless approximates our results within reasonable limits.

More extreme residual motion was reported by Chuang *et al*. (9) in an analysis of six treatments with the CK at different locations throughout the spine, using fiducial implants. They applied a similar approach to ours but defined residual targeting error as the *average* motion between successive kV X-ray image acquisitions (as opposed to *total* motion, which we used). This should have yielded calculated error values about half of what we obtained. Curiously, Chuang *et al*. reported much higher targeting errors than other CK groups (14, 16), which they claimed led to a radial shift of the dose distribution of at least 1.6 mm for one of the cases. We have not found such extensive motion in any of our 260 cases despite using a more conservative approach for error calculation. Even in our maximum motion scenario, a much lower dose discrepancy was found than that reported by Chuang *et al*. (9). We have carefully screened our treatment log data for couch movement and treatment breaks, which can potentially introduce incorrect events of excessive patient motion into the analysis.

We found little difference in the residual patient motion for different sections of the spine, with the exception of roll rotations. We attribute the high roll stability in treatments of the upper cervical spine to the use of a thermoplastic mask for head stabilization. Increased roll shifts in the thoracic and upper lumbar spine can be explained by a small contribution of respiratory motion, which may also account for the slightly higher motion in L/R direction. Roll movements in the lumbar vertebrae 4 and 5 are restrained by their stabilizing proximity to the pelvic bone.

Margin considerations

For more than 95% of our spinal treatments, individual beams were shifted by less than 1 mm on average. The geometric impact on the dose distribution was much lower because of the large number of beams delivered from a wide range of incident angles, as we have established by recalculation of dose volumes for an average and a maximum motion scenario. As a consequence, the addition of margins to compensate for residual patient motion in CK spinal treatments with skeletal structure tracking is not warranted.

Although the raw tracking data in treatments of distant pelvic/sacral lesions concurs with spinal treatments of the lumbar vertebrae 4 and 5, the impact of rotations on the total targeting error for targets far from the tracking center is much higher. Therefore, we recommend applying an additional safety margin of about 2 mm to compensate for residual motion and the targeting uncertainty due to limited mobility in the lumbosacral and sacroiliac joints, as has recently been discussed in detail (17).

CONCLUSIONS

Robotic radiosurgery with the Cyberknife allows for automatic correction of incident beam angles with regard to the current patient position. For this setup, we have provided technical and clinical evidence that submillimeter targeting precision can be achieved in single-session spinal treatments despite of intrafraction patient motion when using a noninvasive fiducial-free tracking technique. Therefore, we consider fiducial implantations obsolete for spinal radiosurgery.

REFERENCES

1. Agazaryan N, Tenn SE, Desalles AA, *et al*. Image-guided radiosurgery for spinal tumors: Methods, accuracy and patient intrafraction motion. *Phys Med Biol* 2008;53:1715–1727.
2. Gutfeld O, Kretzler AE, Kashani R, *et al*. Influence of rotations on dose distributions in spinal stereotactic body radiotherapy (SBRT). *Int J Radiat Oncol Biol Phys* 2009;73:1596–1601.
3. Jin JY, Ryu S, Rock J, *et al*. Evaluation of residual patient position variation for spinal radiosurgery using the Novalis image guided system. *Med Phys* 2008;35:1087–1093.
4. Murphy MJ. Intrafraction geometric uncertainties in frameless image-guided radiosurgery. *Int J Radiat Oncol Biol Phys* 2009;73:1364–1368.
5. Huntzinger C, Munro P, Johnson S, *et al*. Dynamic targeting image-guided radiotherapy. *Med Dosim* 2006;31:113–125.
6. Murphy MJ. An automatic six-degree-of-freedom image registration algorithm for image-guided frameless stereotaxic radiosurgery. *Med Phys* 1997;24:857–866.
7. Fu D, Kuduvalli G, Maurer CR, *et al*. 3D target localization using 2D local displacements of skeletal structures in orthogonal X-ray images for image-guided spinal radiosurgery. *Int J CARS* 2006;1:189–200.
8. Muacevic A, Staehler M, Drexler C, *et al*. Technical description, phantom accuracy, and clinical feasibility for fiducial-free frameless real-time image-guided spinal radiosurgery. *J Neurosurg Spine* 2006;5:303–312.
9. Chuang C, Sahgal A, Lee L, *et al*. Effects of residual target motion for image-tracked spine radiosurgery. *Med Phys* 2007;34:4484–4490.
10. Gerszten PC, Burton SA. Clinical assessment of stereotactic IGRT: Spinal radiosurgery. *Med Dosim* 2008;33:107–116.
11. Tsai JT, Lin JW, Chiu WT, *et al*. Assessment of image-guided CyberKnife® radiosurgery for metastatic spine tumors. *J Neurooncol* 2009.
12. Murphy MJ. Fiducial-based targeting accuracy for external-beam radiotherapy. *Med Phys* 2002;29:334–344.
13. Ho AK, Fu D, Cotrutz C, *et al*. A study of the accuracy of Cyberknife spinal radiosurgery using skeletal structure tracking. *Neurosurgery* 2007;60:147–156.

14. Hoogeman MS, Nuyttens JJ, Levendag PC, *et al*. Time dependence of intrafraction patient motion assessed by repeat stereoscopic imaging. *Int J Radiat Oncol Biol Phys* 2008;70:609–618.
15. Kim S, Jin H, Yang H, *et al*. A study on target positioning error and its impact on dose variation in image-guided stereotactic body radiotherapy for the spine. *Int J Radiat Oncol Biol Phys* 2009;73:1574–1579.
16. Murphy MJ, Chang SD, Gibbs IC, *et al*. Patterns of patient movement during frameless image-guided radiosurgery. *Int J Radiat Oncol Biol Phys* 2003;55:1400–1408.
17. Muacevic A, Drexler C, Kufeld M, *et al*. Fiducial-free real-time image-guided robotic radiosurgery for tumors of the sacrum/pelvis. *Radiother Oncol* 2009. doi:10.1016/j.radonc.2009.05.023.